Chapter 41
Motion Artifact Reduction in Electrocardiogram Using Adaptive Filtering Based on Skin-Potential Variation Monitoring

Shumei Dai, Dongyi Chen, Fan Xiong, and Zhenghao Chen

41.1 Introduction

Cardiovascular diseases have become more and more important in recent years. In the field of clinical and medical research, a standard commercial Ag/AgCl electrode is used to record ECG signal. This electrode contains an electrolyte gel, which can irritate the human skin, and the signal quality degrades over time due to the dehydration of the gel [1, 2]. For this reason, Ag/AgCl electrodes are not suitable for wearable health care devices which are intended for long-term continuous monitoring. Therefore, textile-based dry electrodes are alternatively used owing to their stable electrical properties. Textile electrodes are dry, free from gel, and can be readily converted into wearable medical garments, which make them preferable for long-term monitoring [3].

However, the biggest challenge of the fabric dry electrodes is that the collected ECG signals are greatly disturbed by motion artifacts. Most of the noise can be filtered out using common filtering techniques, but motion artifacts are difficult to filter out since they have the same frequency range as ECG signals. Accurate detection of a person's biopotential signals in movement state is always difficult and challenging [4]. SPV is a major composition of the motion artifacts [5].

The performance of adaptive filtering in noise suppression depends largely on the level of correlation between the reference signal and the ECG noise source [6]. The reference signal measures motion artifacts by means of various sensors (pressure sensors, accelerometers, and optical displacement sensors) [7–10]. A low correlation with motion artifacts were shown in indirectly measured reference

S. Dai · D. Chen (✉) · F. Xiong · Z. Chen
University of Electronic Science and Technology of China, School of Automation Engineering, Chengdu, China
e-mail: dychen@uestc.edu.cn

C. Sugimoto et al. (eds.), *13th EAI International Conference on Body Area Networks*, EAI/Springer Innovations in Communication and Computing,
https://doi.org/10.1007/978-3-030-29897-5_41

signals, because they yield inaccurate estimates of the electrical characteristics of the skin/electrode interface. Ko et al. [11] designed an acquisition structure to measure the half-cell potential by using sol-gel foams wet electrodes, The half-cell potential signal was used to estimate motion artifacts, but wet electrodes were not suitable for long-term use. In general, these research works can effectively reduce motion artifacts by using adaptive filtering. However, the ECG signal collected by the textile electrodes and the motion artifact induced by skin-potential variation (SPV) were not taken into consideration.

In this chapter, a simple method was demonstrated to measure skin-potential variation (SPV). SPV signals were used as reference signals to reduce ECG motion artifacts with the adaptive filtering technique. To measure SPV signal, two additional textile electrodes were positioned adjacent to the ECG sensing electrodes and connected with a resistance. The skin deformation causes a potential difference between the two electrodes, and a voltage drop is generated across the resistance. This voltage drop signal is adaptively filtered as a reference signal input. This method can eliminate the need for placing different sensors on the body, and obtain SPV signal which is high similar with ECG signal by using two more textile electrodes to estimate motion artifacts with adaptive filtering.

41.2 Methodology and Measurement

The proposed method using textile electrodes acquired two types of physiological signals, ECG signals and SPV signals. Then formula derivation, circuit simulation, and experiments were carried on to demonstrate that motion artifacts can be effectively removed by the SPV signal.

Electrical Circuit Model

The equivalent circuit model for ECG signal is shown in Fig. 41.1a, b shows the equivalent circuit model for SPV signal [11]. Z_{si} is the impedance of skin, Z_{ei} is the impedance of skin–electrodes interface, Z_r is the resistance which connects two electrodes, and Z_{in} is the input impedance of the front-end.

In Fig. 41.1a:

$$\mathrm{ECG} = V_1^+ \times \frac{Z_{in}}{Z_{s1} + Z_{e1} + Z_{in}} - V_1^- \times \frac{Z_{in}}{Z_{s2} + Z_{e2} + Z_{in}} \tag{41.1}$$

From Eq. (41.1), when the input impedance Z_{in} is large relatively to the interface impedance ($Z_{s1} + Z_{e1}$, $Z_{s2} + Z_{e2}$) and the impedance between the two lead electrodes is approximately equal ($Z_{s1} + Z_{e1}$, $Z_{s2} + Z_{e2}$), the equation is

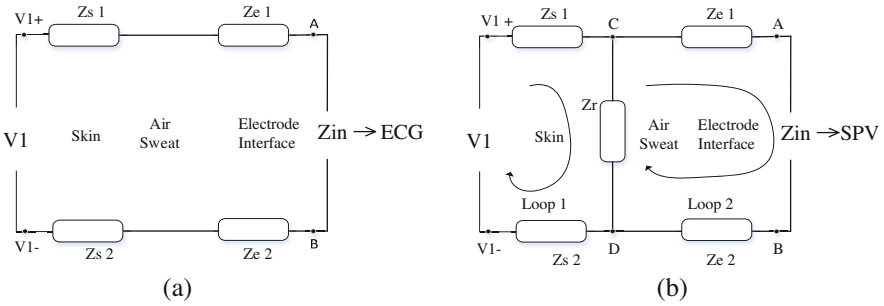

Fig. 41.1 Equivalent circuit model for (**a**) ECG signal; (**b**) SPV signal

approximately equal to ECG $= V_1^+ - V_1^-$. In conclusion, when the front-end input impedance is large relative to the interface impedance, the motion artifacts caused by the impedance change have little effect on the ECG.

In Fig. 41.1b:

$$C - D = \left(V_1^+ - V_1^-\right) \times \frac{Z_r}{S_{s1} + Z_{s2} + Z_r} \cong \quad \text{if} \quad \frac{Z_r}{Z_{s1} + Z_{s2}} \cong 0 \tag{41.2}$$

In Eq. (41.2), when the impedance Z_r is smaller than the interface impedance $Z_{s1} + Z_{s2}$, the equation is close to 0.

$$\text{SPV} = C - D = Z_{in} \times \frac{C - D}{Z_{e1} + Z_{e2} + Z_{in} + Z_r} = \left(\frac{1}{1 + \frac{Z_{e1}+Z_{e2}+Z_r}{Z_{in}}}\right) \times (C - D) \tag{41.3}$$

In formula (41.3), C and D represent skin potentials which are in contact with the electrodes. When $\left(\frac{1}{1+\frac{Z_{e1}+Z_{e2}+Z_r}{Z_{in}}}\right)$ approaches to 1, the SPV is approximate to $C - D$.

Circuit Simulation

First, by using a circuit simulation Software Multisim13.0, the ECG signal acquisition equivalent circuit model and SPV signal acquisition equivalent circuit model were built. Then the influence of impedance change was simulated. The R and the C component values used in the circuit were obtained from previous experiments. The feasibility of the proposed method was evaluated by changing the value of Z_r.

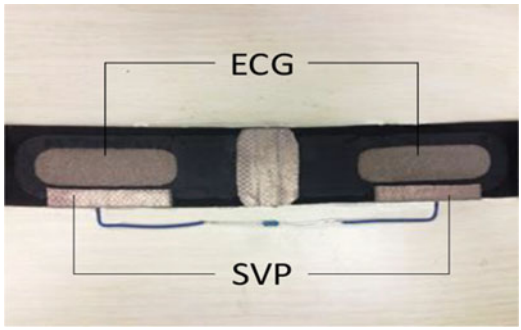

Fig. 41.2 Wearable chest strap

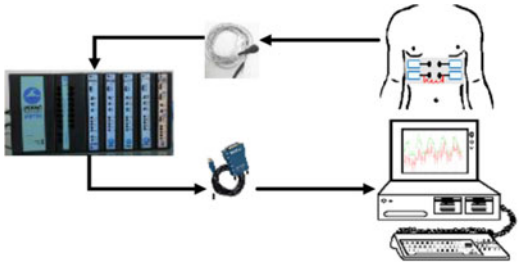

Fig. 41.3 Signal acquisition process

Experiment

The wearable chest strap is shown in Fig. 41.2; two pairs of textile electrodes are integrated on a wearable chest strap, one for ECG signal acquisition, and the other for SPV signal acquisition. Resistance (1, 22, 47, 100 kΩ) connects two textile electrodes which are used to obtain SPV signal connection. The experiment required six male volunteers (A–F) aged 20–25 years old to wear the wearable chest strap under the pressure of 2 N/cm^2, which was fixed at about 1 cm below the chest. The subjects performed stoop motions in an environment of 25 °. ECG signal and SPV signal were measured by BIOPAC data acquisition system (Model: MP36, BIOPAC Systems Inc., USA) with a sample rate of 2000 Hz and 10 s for each recording with the change of the resistance. Biological signals are finally analyzed and processed by a computer. The signal acquisition process is shown in Fig. 41.3.

41.3 Result and Discussion

Circuit Simulation Result

The simulation results are shown in Fig. 41.4 (red: ECG signal, green: SPV signal). As the resistance Z_r decreases, the amplitude of the SPV signal decreases. Obviously, the value of Z_r is very important. When Z_r is smaller than the interface

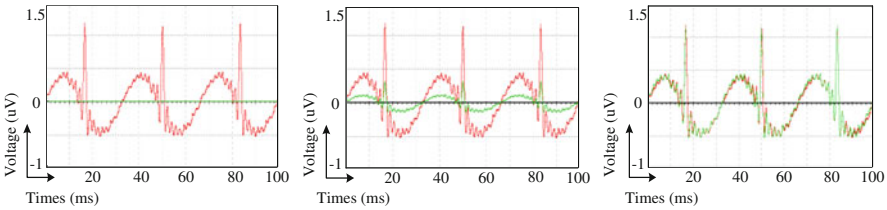

(a) $Zr = 0\Omega$ (b) $Zr = 47k\Omega$ (c) $Zr = 500M\Omega$

Fig. 41.4 Circuit simulation to evaluate the influence of Z_r. (**a**) $Z_r = 0\ \Omega$, (**b**) $Z_r = 47\ k\Omega$, (**c**) $Z_r = 500\ M\Omega$

Table 41.1 The correlation of SPV signal and ECG signal in different resistance values of six males

Resistance value (kΩ)	Correlation of A	Correlation of B	Correlation of C	Correlation of D	Correlation of E	Correlation of F
1	0.3916	0.2665	0.0874	0.0915	0.0862	0.1282
22	0.5170	0.3483	0.2075	0.3291	0.1970	0.2366
47	0.5709	0.7563	0.8626	0.3890	0.2767	0.3684
100	0.4519	0.7088	0.8181	0.1431	0.1622	0.1164

impedance of $Z_{s1} + Z_{s2}$ and $Z_r/Z_{s1} + Z_{s2}$ is approximate to 0, so the SPV signal is close to 0. The effect is shown in Fig. 41.4a, b is the waveform diagram of the ECG signal and the SPV signal when Z_r is 47 kΩ. The SPV signal is superimposed with a weak ECG signal and needs to be removed by preprocessing. As shown in Fig. 41.4c, when Z_r is too large, the path is equivalent to broken circuit and the SPV signal approaches to the ECG signal.

Experimental Result

In the dynamic situation, Table 41.1 shows six volunteers' correlations between the SPV signal and the ECG signal in different value of resistance. When the value of resistance is equal to 47 kΩ, the SPV signal and the ECG signal have a highest correlation.

Adaptive filtering was conducted using a basic LMS (least mean square) error cancellation algorithm, and the SPV signal measured in four resistances are respectively input as adaptive filtering reference signal. The output of adaptive interference cancellation is shown in Fig. 41.5. It can be seen that the ECG signal and SPV signal in the 47 kΩ resistance have a high correlation, and the wave fluctuation of two signals is consistent. Table 41.2 shows the changes of SNR before and after the interference cancellation. As shown in Fig. 41.5 and Table 41.1, when the SPV signal measured in 47 kΩ resistance is used as a reference signal, the filtered QRS waveform is obvious and the SNR is improved.

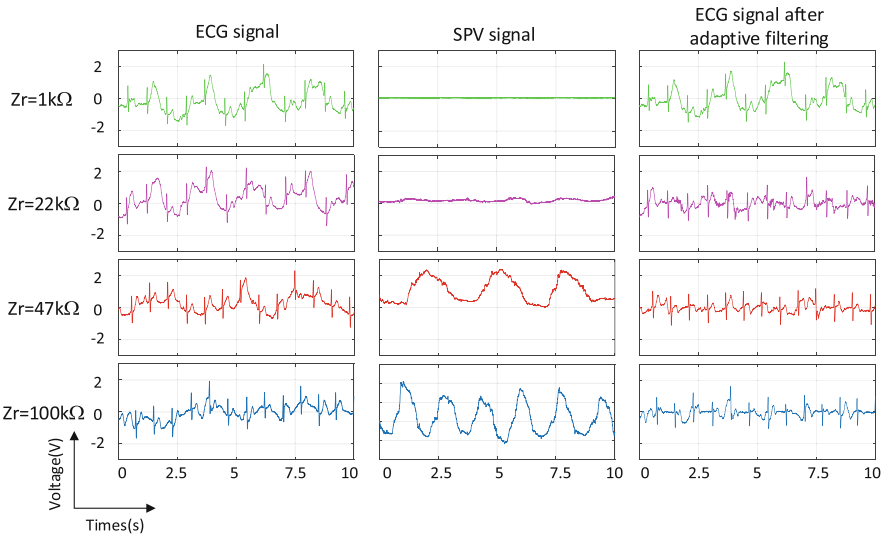

Fig. 41.5 ECG waveforms before and after adaptive filtering in different resistances

Table 41.2 The SNR changes of ECG signals with SPV interference in different resistance values

Resistance value (kΩ)	Before filtering SNR (dB)	After filtering SNR (dB)	SNRI (dB)
1	5.7453	5.8274	0.0821
22	5.7947	8.7272	2.9325
47	6.0317	11.7578	5.7261
100	5.5763	10.4293	4.8530

Independent component analysis is one of the recently developed techniques for the blind source separation (BSS). It is used to identify original signals from the observed linear combinations of the original signals. We deal with the ECG signals by using adaptive filtering algorithm and ICA algorithm, and the adaptive filtering reference signal is the SPV signal in 47 kΩ resistance. The output of filtering is shown in Fig. 41.6. Table 41.3 shows that adaptive filtering has higher SNR values and better noise suppression than ICA filtering.

The results demonstrate the feasibility of the method by using textile electrodes to measure the SPV signal as an adaptive filtering reference signal, and the results show the ability of adaptive filtering in suppression of motion artifacts in electrocardiograms recorded with textile electrodes.

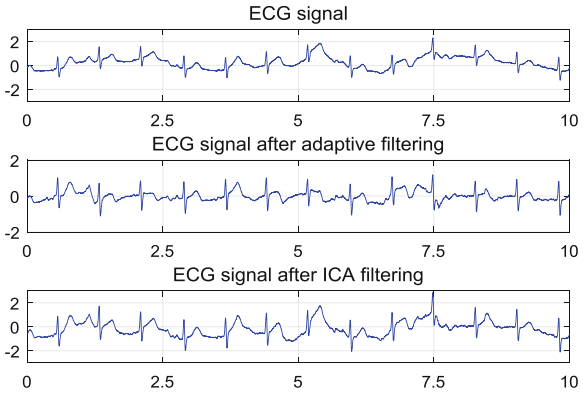

Fig. 41.6 ECG waveforms after adaptive filtering of different resistances

Table 41.3 The SNR changes of adaptive filtering and ICA filtering

Algorithm name	Before filtering SNR (dB)	After filtering SNR (dB)	SNRI (dB)
Adaptive filtering	6.0317	11.7578	5.7261
ICA filtering	6.0317	7.1343	1.1026

41.4 Conclusion

In this chapter, the SPV signal acquisition structure can effectively measure the skin-potential variation. The SPV signal is measured by textile electrodes and served as a reference signal for adaptive filtering. In this way, it can effectively remove the motion artifact caused by the skin-potential variation. Since two electrode pairs are distributed on the same substrate and the acquisition position of two signals is close, the motion artifact can be measured more accurately, ensuring the high correlation between ECG and SPV signals. Besides, using the electrode to collect the SPV signal doesn't require extra sensor components and improves the accuracy of the later diagnosis.

It can be found in the experiments that the correlation between the SPV signal and the ECG signal is deteriorated when large movements, such as running and jumping, are performed, which leads to insignificant signal characteristics after filtering. In the future, researchers should focus on removing motion artifacts under large-scale motions.

Acknowledgments This work is supported by National Natural Science Foundation of China (no. 61572110) and National Key Research & Development Plan of China (no. 2016YFB1001401).

References

1. Chi, Y.M., Jung, T.-P., Cauwenberghs, G.: Dry-contact and noncontact biopotential electrodes: methodological review. IEEE Rev. Biomed. Eng. **3**, 106–119 (2010)
2. Yao, S., Zhu, Y.: Nanomaterial-enabled dry electrodes for electrophysiological sensing: a review. JOM. **68**(4), 1145–1155 (2016)
3. Xu, P.J., Zhang, H., Tao, X.M.: Textile-structured electrodes for electrocardiogram. Text. Prog. **40**(4), 183–213 (2008)
4. Wiese, S.R., et al.: Electrocardiographic motion artifact versus electrode impedance. IEEE Trans. Biomed. Eng. **52**(1), 136–139 (2005)
5. Weihua, P., et al.: Skin-potential variation insensitive dry electrodes for ECG recording. IEEE Trans. Biomed. Eng. **64**(2), 463–470 (2017)
6. Lu, G., et al.: Removing ECG noise from surface EMG signals using adaptive filtering. Neurosci. Lett. **462**(1), 14–19 (2009)
7. Pengjun, X., Xiaoming, T., Shanyuan, W.: Measurement of wearable electrode and skin mechanical interaction using displacement and pressure sensors. In: 2011 4th International IEEE Conference on Biomedical Engineering and Informatics (BMEI), vol. 2, 2011
8. Tong, D.A.: Electrode systems and methods for reducing motion artifact. U.S. Patent No. 6,912,414, 28 Jun 2005
9. Tong, D.A., Bartels, K.A., Honeyager, K.S.: Adaptive reduction of motion artifact in the electrocardiogram. In: Proceedings of the Second Joint. IEEE Engineering in Medicine and Biology, 2002. 24th Annual Conference and the Annual Fall Meeting of the Biomedical Engineering Society EMBS/BMES Conference, 2002, vol. 2, 2002
10. Liu, Y., Pecht, M.G.: Reduction of skin stretch induced motion artifacts in electrocardiogram monitoring using adaptive filtering. In: Engineering in Medicine and Biology Society, 2006. EMBS'06. 28th Annual International Conference of the IEEE, IEEE, 2006
11. Byung-hoon, K. et al.: Motion artifact reduction in electrocardiogram using adaptive filtering based on half cell potential monitoring. In: 2012 Annual International Conference of the IEEE Engineering in Medicine and Biology Society (EMBC), 2012